Proceedings of the
International Conference on Mechanical Engineering 2003
(ICME2003) 26- 28 December 2003, Dhaka, Bangladesh

ICME03-FL-08

A STUDY OF THE A-PILLAR VORTEX OF A PASSENGER CAR

Firoz Alam[1], **Gary Zimmer**[2] **and Simon Watkins**[1]

[1]School of Aerospace, Mechanical and Manufacturing Engineering
RMIT University
PO Box 71, Bundoora, Melbourne, VIC 3083, AUSTRALIA

[2]School of Science and Technology
Ballarat University, Ballarat, AUSTRALIA

ABSTRACT

The flow separation around the A-pillar of a passenger car is a dominant source of aerodynamic noise and surface pressure fluctuations on the front side window glass. Aerodynamically generated noise adversely affects vehicle occupant's comfort. Many modern cars still have high fluctuating exterior hydrodynamic pressure due to flow separation in the A-pillar region. The size and magnitude of the A-pillar flow separation mainly depend on the local A-pillar and windshield geometry and yaw angles. The purpose of this paper is to investigate how these fluctuations vary with local geometry and Reynolds number.

Keywords: Wind noise, A-pillar, Reynolds number, Pressure coefficient, Wind tunnel, Yaw angle

1. INTRODUCTION

Studies by Alam [1, 2], Haruna et al. [3], Hucho [4], Popat [5], Watanabe and Harita [6] and Zimmer et al. [7] have shown that the fluctuating pressures in the A-pillar region of a passenger car are the primary source of aerodynamic noise as strong flow separation occurs here due to complex A-pillar geometry. A-pillar of a car can be defined as the structural joint between the windshield and front side window. Aerodynamic noise adversely affects occupant's comfort as other sources of noise (e.g., engine, transmission and road/tyre interaction noise) are less dominant at high speeds (100 km/h and over). High aerodynamic noise levels can not only make it difficult for vehicle occupants to converse or listen to the radio but also cause driver fatigue on a long highway trip. Due to the flow separation in the A-pillar region, a rotational vortex is formed in the A-pillar region and it expands and travels towards the roof. This conical vortex generates not only acoustic waves but also causes side window to vibrate and radiate noise into the interior of the vehicle. Many modern cars still have high fluctuating exterior hydrodynamic pressure due to flow separation in the A-pillar region. The size and magnitude of the A-pillar flow separation mainly depend on the local A-pillar and windshield geometry and yaw angles. The primary objectives of this work are to investigate the effects of A-pillar geometry on the potential for noise generation of production vehicles. For this purpose, two current production passenger cars were used and one of the car's front side window was fitted with flush mounted microphones and pressure taps to measure surface fluctuating and mean pressures. Testing was conducted at RMIT University Industrial Wind Tunnel, Monash/RMIT Universities' Aeroacoustic Wind Tunnel and on-road. However, the results from Monash/RMIT Universities' Wind Tunnel will be presented in this work. The production vehicle was tested with the vehicle in factory trim (i.e., standard configuration) and also with the modification of the A-pillar region. Flow structure around the A-pillar region was documented using flow visualization.

2. EXPERIMENTAL PROCEDURE

As mentioned earlier, in order to assess the effects of increased rounding of the A-pillar of a production vehicle on the 'in-cabin noise' and surface flow, two current production vehicles were tested in the wind-tunnel. These two vehicles were a General Motors-Holden (GMH) VR Commodore station wagon and a VT Calais sedan (see Figures 4 and 5). Both cars were locally manufactured by GMH Australia. The VR Commodore was a five door station wagon and VT Calais was a four-door family sedan. These vehicles are similar to many large family-size cars mass produced around the world including North America, Europe and Australia.

The initial test was conducted to visualize the flow around the A-pillar region with wool tufts using the VR Commodore station wagon. The vehicle was tested at a range of speeds (40 km/h to 140 km/h with an increment of 20 km/h) with standard configuration (without side rear view mirror) and with modified A-pillar (with a removable fibre-glass modified A-pillar cover that provided a smooth radius over the A-pillar (see Figure 5).

The VT Calais was used to measure the surface mean and fluctuating pressures on the side glass in the A-pillar region using a multi-channel Scannivalve pressure

scanning device and ¼ inch diameter condenser microphones. Problems found drilling a production toughened glass side window did not permit measurement of surface mean and fluctuating pressures on a production window. However, this was overcome by using a four-millimeter thick Perspex side window mounted so that the curvature approximated the production window. The Perspex could be easily drilled for mounting the pressure taps and microphones. The surface mean and fluctuating pressures were measured at 16 locations (8 holes of 2 rows). The horizontal spacing was 80 mm and the position of these two rows from the window belt line was 1/3 and 2/3 the glass height (see Figure 6). For more details, refer to the PhD Thesis by Zimmer [8]. Microphones were flush mounted on the surface at the same location where surface mean pressure taps were. Microphones were embedded within the circular adaptors (not shown here) and mounted flush with the surface. They were connected to a 16 channel Digital Audio Tape recorder (SONY PC 216A). All microphones were calibrated before and after the measurements via a Piston phone calibrator. Signals from the microphones were continuously checked with an oscilloscope during the recording. A 10-second sample (out of a 30-second record) obtained at 48,000 Hz was analysed to calculate the non-dimensional fluctuating pressure coefficients (Cp rms), using the following relationship ($C_{p\,rms}=\frac{p_{std}}{\frac{1}{2}\rho V^2}$), where p_{std} is the standard deviation of the fluctuating pressure and $\frac{1}{2}\rho V^2$ is the mean velocity head (q) and spectral characteristics. The mean velocity head was obtained from the tunnel data acquisition system. The time-averaged pressure distributions were then converted to the non-dimensional pressure coefficients (Cp), using the following relation: $C_p=\frac{p_m-p_\infty}{\frac{1}{2}\rho V_\infty^2}$. Here p_m is the time-averaged surface pressure on the side window near the A-pillar), p_∞ is the free stream static pressure and V_∞ is the free stream velocity.

As mentioned earlier, tests were conducted at the Monash/RMIT Universities' Aeroacoustic Wind Tunnel, which is an open jet wind tunnel with a maximum speed of approximately 180 km/h. It is run jointly by Monash University and RMIT University and located at the Clayton Campus of Monash University. The exit nozzle size is 10.55 metres square and the test section has very low levels of background noise. The test section has a turntable and is large enough to accommodate a full-size car and bread delivery van. The tunnel is driven by two independently controlled fans of 5-m diameter. It consumes approximately 2 MW power (see Figures 1, 2 and 3). The tunnel's air speeds were measured via two modified NPL ellipsoidal head Pitot-static tubes connected to two MKS Baratron Pressure sensors through flexible tubing.

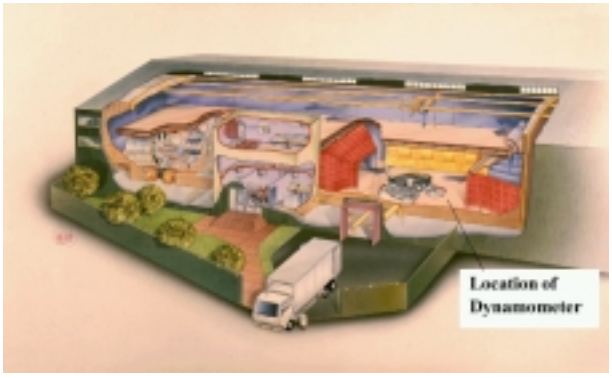

Fig 1. An Artistic View of Monash/RMIT Universities' Aeroacoustic Wind Tunnel

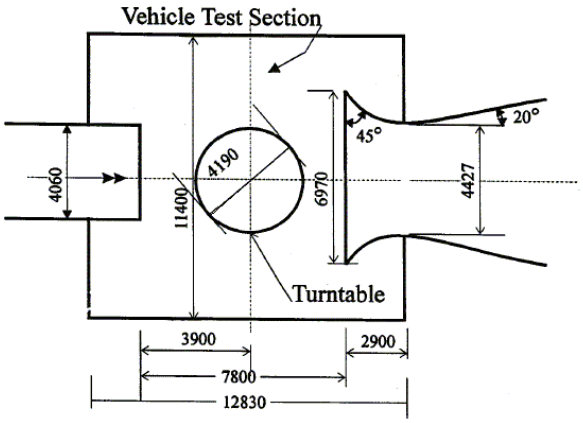

Fig 2. A Plan View of Monash/RMIT Wind Tunnel Test Section

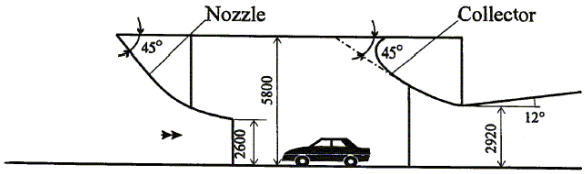

Fig 3. A Side View of Monash/RMIT Wind Tunnel Test Section

Fig 4. General Motors-Holden VT Calais with Modified A-pillar at Monash/RMIT Universities' Wind-Tunnel

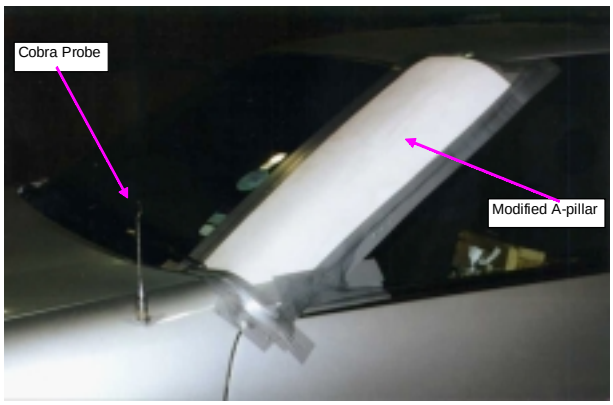

Fig 5. General Motors-Holden VR Commodore Station Wagon with Modified A-pillar and Cobra Probe

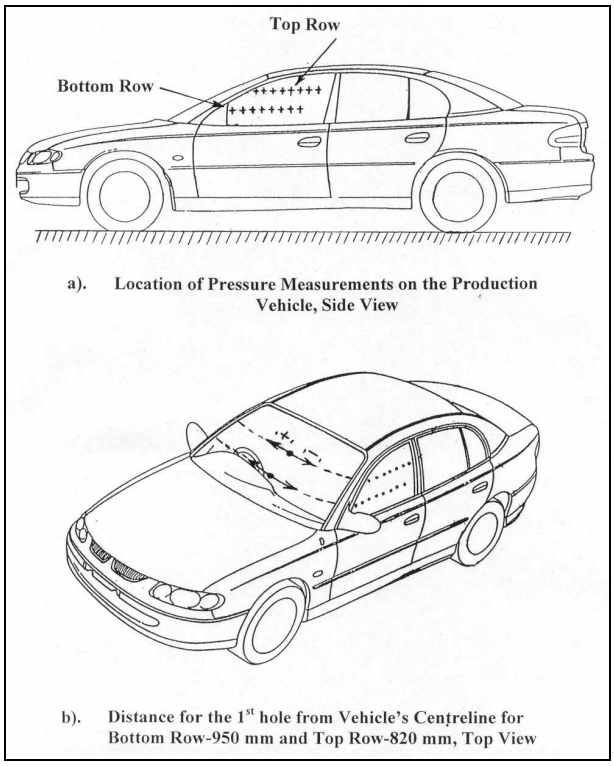

Fig 6. A Schematic of Data Presentation in Relation to Vehicle's Centre Line (VT Commodore)

3. RESULTS AND DISCUSSION

Visualised flow and surface mean and fluctuating pressure coefficients for all speeds tested at zero yaw angles are shown and discussed. The results for other yaw angles are not presented here. The surface mean and fluctuating pressure coefficients are plotted against the distance from the line of symmetry (at the front) of the production vehicle (for details of how the graphical results relate to the model geometry, refer to Figure 6).

3.1 Effects of Modified A-pillar on Surface Mean Pressure

The surface mean pressure coefficient variation with distance along the side window near the A-pillar from the centre-line of the vehicle is shown in Figures 9 to 12. No significant effects of Reynolds numbers on the surface mean pressure coefficients (for the standard and modified A-pillar) are evident (see Figures 9 and 10).

The flow structure on the front side glass around the A-pillar region is very complex. A spiral vortex is formed close to the A-pillar edge. Figure 7 shows a strong conical vortex existed along the A-pillar edge on the side window and the vortex flow was unsteady. The flow visualisation photographs (Figures 7 and 8) showed that the modified A-pillar had a significant influence on the flow structures in the A-pillar region. However, the flow visualisation photograph of the modified A-pillar (Figure 8) indicates that the flow was mostly attached and the A-pillar vortex almost disappears.

The increased rounding (stream-ling) of the A-pillar has a significant effect on the A-pillar flow structures. The plot for surface mean pressure coefficients for the modified A-pillar supports this. Increased rounding reduces the magnitude of surface mean pressure (see Figures 9 and 10). It may be noted that unavoidably, the first two positions at each row (top and bottom) close to the A-pillar edge were covered by the modified A-pillar. Therefore, the data presented here were from the 12 positions (2 rows of 6).

Fig 7. Side View of Flow Visualisation with Standard A-pillar, Yaw = 0°, Speed = 100 km/h

Fig 8. Side View of Flow Visualisation with Modified A-pillar, Yaw = 0°, Speed = 100 km/h

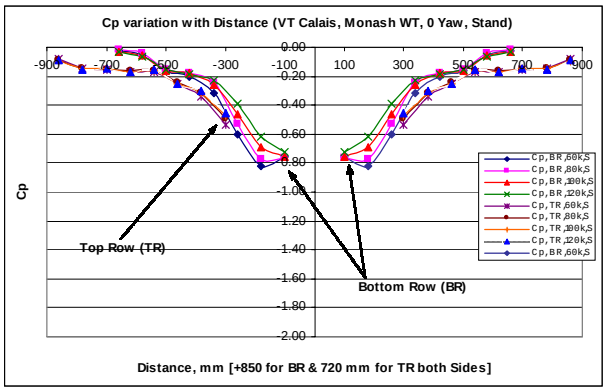

Fig 9. Surface Mean Cp Variation with Distance, Yaw = 0° (Standard A-pillar)

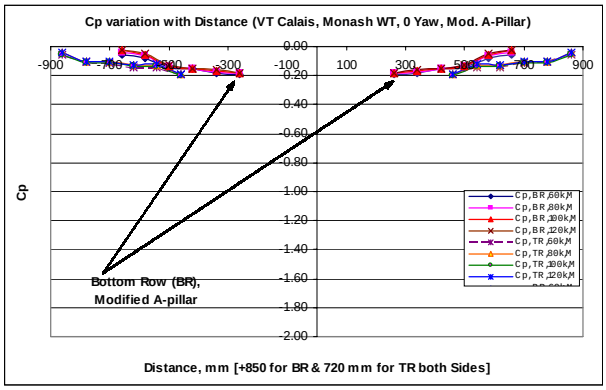

Fig 10. Surface Mean Cp Variation with Distance, Yaw = 0° (Modified A-pillar)

3.2 Effects of Modified A-pillar on Surface Fluctuating Pressure

The fluctuating pressure coefficients (Cp rms) variation with distance for the standard and modified A-pillar are shown in Figures 11 and 12. No significant variation of Reynolds numbers on the surface fluctuating pressure coefficients (standard and modified A-pillar) is evident. The increased radius of the A-pillar due to modification reduces the magnitude and size of the A-pillar vortex significantly. This reduction is evident not only at zero yaw but also at other yaw angles (±15º, not shown here). It may be noted that the leeward side is defined as negative yaw angle, which usually generates larger flow separation compared to windward side defined as positive yaw angle.

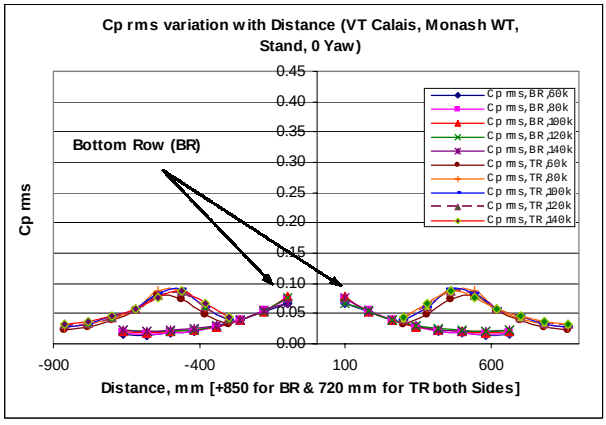

Fig 11. Surface Fluctuating Cp rms Variation with Distance, Yaw = 0° (Standard A-pillar)

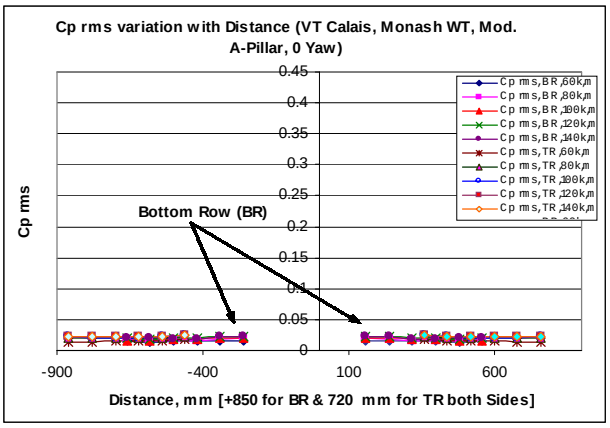

Fig 12. Surface Fluctuating Cp rms Variation with Distance, Yaw = 0° (Modified A-pillar)

3.3 Spectral Analysis of Surface Fluctuating Pressure

The Power Spectral Density (PSD) was used to document the energy characteristics of fluctuating pressures in the frequency domain. In this work, the fluctuating pressure data, from the position where maximum fluctuating pressure was measured (at zero and ±15º) was used for the PSD analysis. The PSD for 0° yaw angle are shown in Figures 13 and 14 for the standard and modified A-pillar for the speed of 140 km/h.

For the standard A-pillar (Figure 13), the fluctuating pressure spectrum contains higher energy compared to the spectrum at zero yaw angles at frequencies below 300 Hz. However, the pressure spectrum at positive yaw angles contains higher energy at frequencies above 300 Hz. The peak energy at negative yaw angles is close to 90 Hz. The spectrum at positive yaw angles contains the lowest energy compared to the spectra at negative and zero yaw angles.

For the modified A-pillar (Figure 14), the spectrum at negative yaw angles possesses highest energy compared to spectra at zero and positive yaw angles. Most energy was noted at low frequencies.

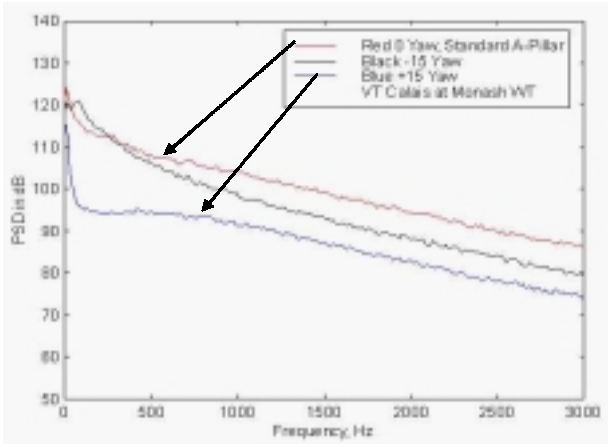

Fig 13. Power Spectra Plot of Peak Cp rms, Yaw = 0°, -15° and +15° (Standard A-pillar)

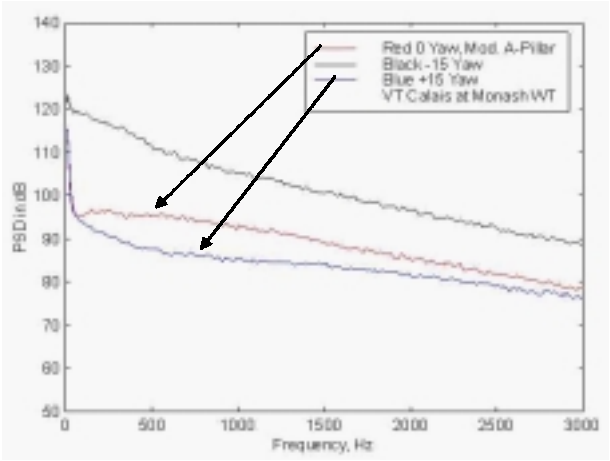

Fig 14. Power Spectra Plot of Peak Cp rms, Yaw = 0°, -15° and +15° (Modified A-pillar

4. CONCLUSIONS

The following conclusions have been drawn from the work presented here:

Simple changes in A-pillar geometry have significant effects on reducing flow separation (thereby reducing the potential for aerodynamic noise) in this area. Frequency based analysis supports the above statement.

There are no significant effects of Reynolds numbers on surface mean and fluctuating pressure coefficients.

5. ACKNOWLEDGEMENTS

The authors would like to express their sincere thanks to the Australian Federal Government for providing APA Scholarships to first and second authors.

6. REFERENCES

1. Alam, F., Zimmer, G. and Watkins, S., 2003, "Mean and time-varying flow measurements on the surface of a family of idealized road vehicles", *Experimental Thermal and Fluid Science*, 27 (2003), pp 639-654, Elsevier Science.
2. Alam, F., 2000, "The effects of Car A-Pillar and Windshield Geometry on Local Flow and Noise", *Ph.D Thesis*, Department of Mechanical and Manufacturing Engineering, RMIT University, Melbourne, Australia.
3. Haruna, S., Nouzawa, T., Kanimoto, I. and Hiroshi, S., 1990, "An Experimental Analysis and Estimation of Aerodynamic Noise Using a Production Vehicle", *SAE Paper No. 900316*.
4. Hucho, W-H. (editor), 1998, "Aerodynamics of Road Vehicles", 4th Edition, *SAE International*, Warrendale, USA.
5. Popat, B. C., 1991, "Study of Flow and Noise Generation from Car A-Pillar, *Ph.D. Thesis*, Department of Aeronautics, Imperial College of Science, Technology and Medicine, University of London, U.K.
6. Watanabe, M. and Harita, M., 1998, "The Effects of Body Shapes on Wind Noise", *SAE Paper No. 780266*.
7. Zimmer, G., Alam, F., Watkins, S. and Peric, C., 2001, "Comparison of a High-Blockage Wind Tunnel, an Open Jet Wind Tunnel, and On-Road with respect to External Surface Pressures" *SAE 2001-01-1087 Technical Paper Series, SAE World Congress*, 5-8 March, Detroit, USA.
8. Zimmer, G., 2003, "The Contribution of the A-pillar Vortex to Vehicle Interior Noise", *PhD Thesis*, Department of Mechanical and Manufacturing Engineering, RMIT University, Melbourne, Australia.

8. NOMENCLATURE

Symbol	Meaning	Unit
V	Velocity	m/s
Cp	Mean Pressure Coefficient	-
Cp rms	Fluctuating Pressure Coefficient	-
Re	Reynolds number	-
P	Pressure	Pa
SPL	Sound Pressure Level	dB
BR	Bottom Row	-
TR	Top Row	-
PSD	Power Spectral Density	